Proceedings of the IASS 2024 Symposium
Redefining the Art of Structural Design
August 26-30, 2024, Zurich, Switzerland
Philippe Block, Giulia Boller, Catherine DeWolf,
Jacqueline Pauli, Walter Kaufmann (eds.)

Transformable Surface Mechanisms based on Bending-active Scissors Structures

Seri NISHIMOTO[a], Tomohiro TACHI[*]

[*] Department of General System Studies, Graduate School of Arts and Sciences, The University of Tokyo
The University of Tokyo, 3-8-1 Komaba, Meguro-ku, Tokyo, Japan
tachi@idea.c.u-tokyo.ac.jp

[a] Department of Architecture, Graduate School of Engineering, The University of Tokyo

Abstract

Deployable structures made of elastic materials connected by rotational pivots that transform from a flat state to a curved surface have advantages such as being lightweight and construction efficiency. In particular, the geodesic grid shell, in which flat members follow the geodesics of the surface, has one degree of freedom for in-plane deformation, which makes its deployment easy to control. In this study, we propose a design method for deployable surface mechanisms based on a combination of bending-active scissors structures. The mechanism transforms into a 3D curved surface due to the incompatibility of the in-plane shear deformation of the scissors' units.

In this paper, we geometrically show that if two states of the same combination of unis exist, they can smoothly transition between them. Using this feature, we propose a design method for a mechanism that can deploy to a target surface by creating two states of equal length. We also present design examples and physical prototypes. Our structure can be efficiently fabricated by the assembly of short, straight members in the 2D state. We believe this method can be applied to deployable structures such as temporary shelters and flexible partitions.

Keywords: transformable structure, bending active scissors, geodesic grid shell, elastic gridshell

1. Introduction

Deployable gridshell structures, which consist of elastically deformable straight members connected by pivot hinges, have advantages such as being lightweight, construction efficiency, and material efficiency. In particular, the geodesic grid shell, in which slats follow the geodesics of the surface, has one degree of freedom for in-plane deformation, which makes its deployment easy to control. The structural principle of such transformable surface mechanisms has been used in the traditional craft of finger traps and modern fashion designs. Our objective is to explore the kinematics of the mechanisms and the surface design where the slats are joined with rotational pivots to make them useful for deployable grid shells and adaptive products.

If we consider the kinematics of the mechanisms connected by rotational pivots, they generally form an overconstrained system in the in-plane deformation. This makes it impossible for the system to create an arbitrary target surface with a single geodesic grid. Pillwein et al. [1] proposed a method to obtain curved surfaces by replacing pivot holes with slits with play and sliding the hinge. However, this method provides additional degrees of freedom and requires the slide hinges to be fixed after deployment. A method without play in hinges is proposed in [2], however, it is kinematically overconstrained, and the member must bend in the in-plane direction before deployment and during the deployment operation. Ono and

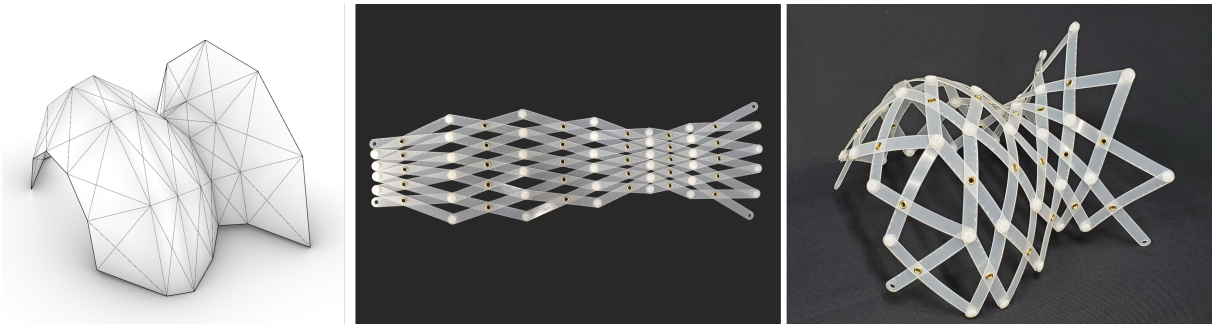

Figure 1: Example of the bending-active scissors mechanism.

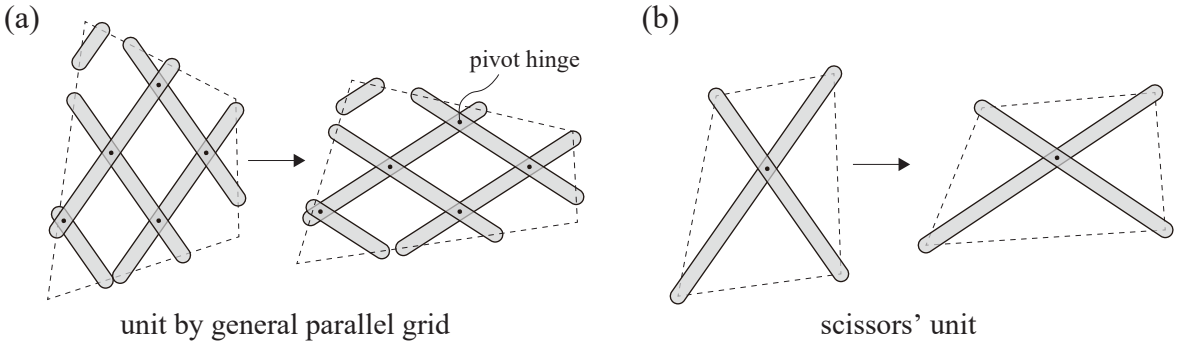

Figure 2: In-plane scissors' transformation of a single grid. (a) unit of the general parallel grid, (b) scissors' unit by quadrilateral diagonals.

Tachi [3] achieved one-degree-of-freedom in-plane deformation by dividing the surface into multiple segments and connecting the scissors' units without play. They generated surfaces with constant negative curvature but were limited to rotationally symmetric shapes because the combination of multiple units is generally overconstrained. Nishimoto and Tachi [4] identified general compatibility conditions for the combination of multiple grids. However, the method of designing the mechanism from the target geometry was limited to the combination of symmetrical shape units that satisfy the compatibility conditions. In addition, the connection of the endpoints of the grid members was problematic, making it difficult to produce a physical model.

This research aims to construct a curved surface mechanism that deploys with one degree of freedom by connecting multiple bending-active geodesic scissors units (Figure1). First, we describe the in-plane deformation of the unit geometrically and show the compatibility conditions for multiple scissors to be valid and have a continuous motion around a vertex. We also clarify that the existence of two states is a necessary and sufficient condition for obtaining continuous mechanisms (Section 2.). Next, using this property, we introduce a design method for mechanisms that can deploy to given target surfaces (Section 3.). We also present examples of actual design and fabrication of mechanisms using the proposed method (Section 4.).

2. Geometry of scissors' transformation

In this paper, we consider the scissors created by the diagonals of a convex quadrilateral as a *unit* (Figure 2 (b)). The authors proposed a mechanism in which units created by cropping parallel grids in arbitrary polygons are connected by edges, in [4] (Figure 2 (a)). The scissors unit considered in this paper can be taken as a special case of a possible unit shape such that the diagonals of the polygon and the interior members are coincident. However, this section's discussion of scale factors can also apply to units that

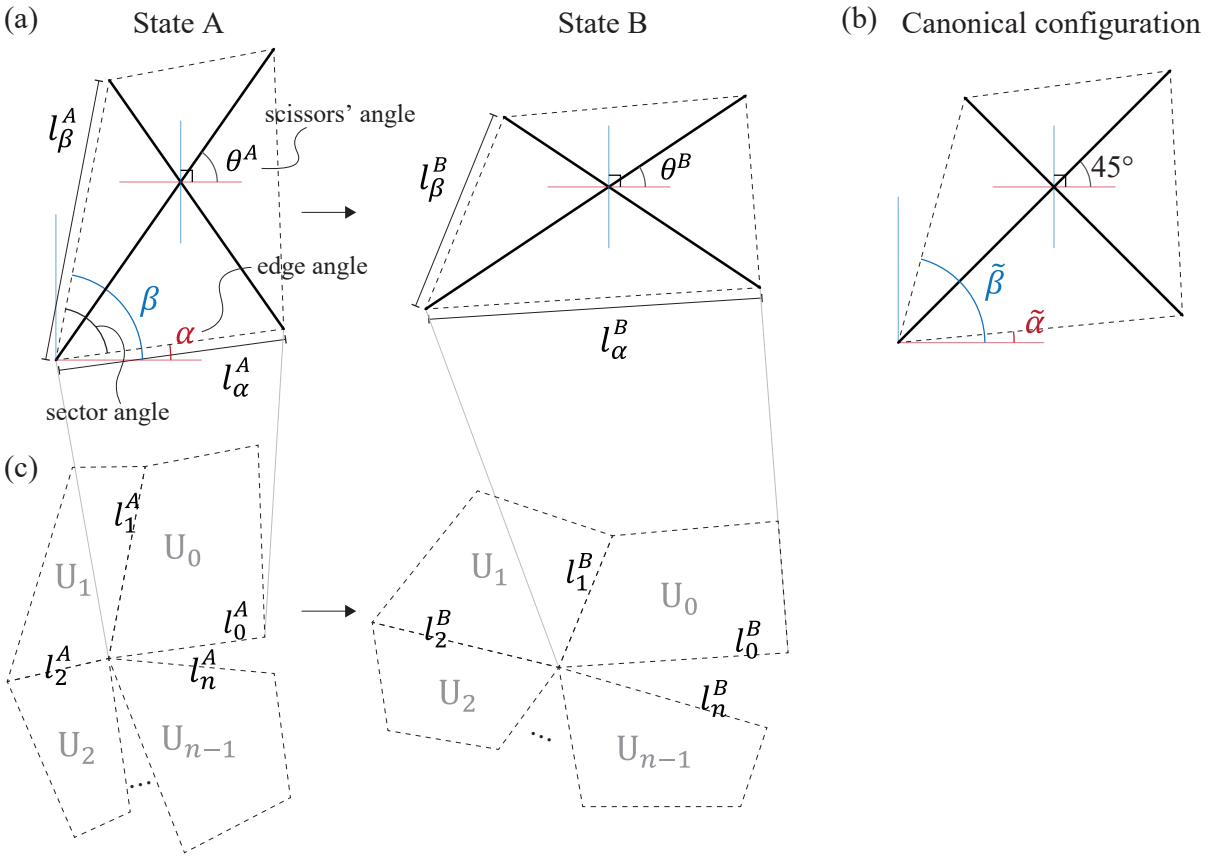

Figure 3: (a) Scissors' transformation of one unit, (b) canonical configuration, (c) n units connection around a vertex.

are cut from general parallel grids.

2.1. Scissors' transformation of single unit

When the scissors' unit transforms in-plane, each edge of the quadrilateral unit expands or contracts. The direction that bisects the member direction is the *principal direction*, and the angle from the principal direction to the member direction is the *scissors' angle* θ. The angle between two consecutive edges of the unit, *sector angle*, changes by changing θ. We let α and β, called *edge angles*, be the angle from the principal direction to the edges, so $|\alpha - \beta|$ is the sector angle between the edges. To represent the direction of the edges independently of the scissors' angle, we use the form with $\theta = 45°$, called the *canonical configuration*, and let $\tilde{\alpha}$, $\tilde{\beta}$ be the edge angles in the canonical configuration (Figure 3(b)).

The scale factor $S_{\tilde{\alpha}}$ of the edge in the direction of the edge angle $\tilde{\alpha}$ when transforming from state A ($\theta = \theta^A$) to state B ($\theta = \theta^B$) can be expressed as follows:

$$S_{\tilde{\alpha}}^2 = \frac{1 + \cos 2\tilde{\alpha} \cos 2\theta^B}{1 + \cos 2\tilde{\alpha} \cos 2\theta^A}. \tag{1}$$

$S_{\tilde{\beta}}$ can be expressed in the same way as Equation (1) using $\tilde{\beta}$, therefore $S_{\tilde{\beta}}$ can be obtaind from $S_{\tilde{\alpha}}$ as follows.

$$S_{\tilde{\beta}}^2 = \frac{-\sec 2\tilde{\alpha} + \sec 2\tilde{\beta} + (\cos 2\theta^A + \sec 2\tilde{\alpha}) S_{\tilde{\alpha}}^2}{\cos 2\theta^A + \sec 2\tilde{\beta}} \tag{2}$$

Since $\tilde{\alpha}$, $\tilde{\beta}$, and θ^A are constant if the parameters of the state A are given, $S^2_{\tilde{\beta}}$ is expressed by the following linear equation.

$$S^2_{\tilde{\beta}} = rS^2_{\tilde{\alpha}} + s \tag{3}$$

where,

$$r = \frac{\cos 2\theta^A + \sec 2\tilde{\alpha}}{\cos 2\theta^A + \sec 2\tilde{\beta}}, \quad s = \frac{-\sec 2\tilde{\alpha} + \sec 2\tilde{\beta}}{\cos 2\theta^A + \sec 2\tilde{\beta}}. \tag{4}$$

From Equation (3), we can obtain the scale factor of one edge from the scale factor of another edge.

2.2. Compatibility between multiple units

When multiple units are connected serially with a common edge, they form a one-DOF mechanism because of the propagation of edge scaling. However, if the connection has an internal vertex, the overall structure is overconstrained because this connection has a closed loop. Therefore, the motion is generally incompatible but can be linked under specific conditions. In the following, we discuss the conditions under which a mechanism becomes compatible around an internal vertex and can be linked as a one-degree-of-freedom mechanism. If it can be linked together, the sum of the sector angles of the units around the vertex increases or decreases, resulting in a transformation from a planar to a three-dimensional surface.

Consider a situation where n units $(U_0, U_1, ..., U_{(n-1)})$ are connected around a vertex (Figure 3(c)) ($i = 0, 1, 2, \ldots, n-1$, modulo n). The scale factor of the edge S_i can be obtained from S_0 as follows.

$$S_i^2 = P_i S_0^2 + Q_i, \tag{5}$$

where,

$$P_i = \prod_{k=0}^{i-1} r_k, \quad Q_i = P_i \sum_{k=0}^{i-1} \frac{1}{P_{k+1}} s_k, \tag{6}$$

where r_k and s_k are obtained as the r and s of each unit k obtained by Equation (4).

The necessary and sufficient condition that the mechanism is valid around the vertex with n unit at state A is that the lengths of the 0th and nth edges are identical ($l_0^A = l_n^A$). In addition, for this to form a continuous mechanism, $S_0 = S_n$ needs to be satisfied for a continuous family of varying S_0. This is equivalent to Equation (5) being identity:

$$P_n = 1, \quad Q_n = 0. \tag{7}$$

2.3. Equivalent condition for multi-vertex structure

For mechanisms with multiple closed vertices, directly finding the parameters of all units that simultaneously satisfy Equation (7) is not straightforward. Instead, we can use the following equivalence of the existence of motion and the existence of states. Since scale factor propagation can be expressed as a linear Equation (3), if there are two states in which the same units are connected in the same relationship, the mechanism can go back and forth between the two states (Figure 4).

This can be explained by using the scale factor as follows. First, suppose that there exist two states in which $S_0 = S_n = 1$ and $S_0 = S_n = S$, respectively. Substituting these values into Equation (5), we obtain the following equation.

$$1 = P_n + Q_n, \text{ and } S^2 = S^2 P_n + Q_n. \tag{8}$$

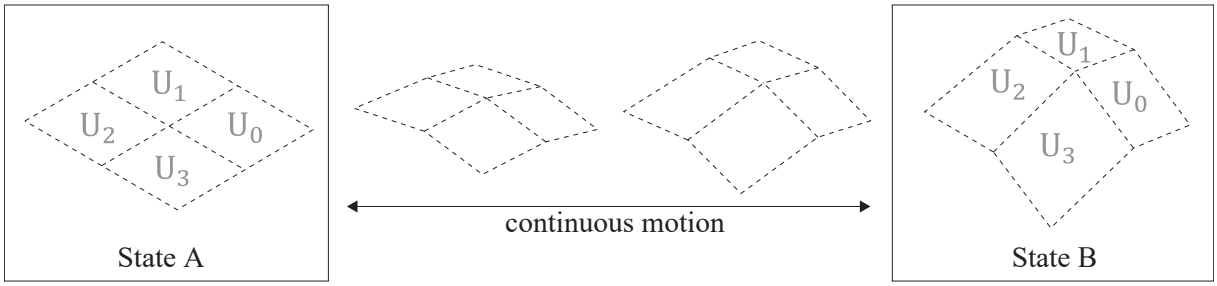

Figure 4: Equivalence between the existence of motion and the existence of states. If two states of the same connection relationship of the same unit exist, there is a continuous motion between them.

From Equation (8), if $S \neq 1$, $P_n = 1$ and $Q_n = 0$ holds, so Equation (7) is satisfied. Therefore, if there are two valid states of the same combination of units, they form a continuous mechanism between two states. In the following design methods, we use this equivalence to computationally find a mechanism by finding two compatible configurations, A and B.

3. Design method

In this section, we propose a method for designing compatible mechanisms by generating two states in which the same units are connected in the same relationship. We implemented a method for designing mechanisms by combining multiple scissors' units and can deploy to a given target surface from a flat state. We used Grasshopper [5] and Kangaroo2 [6] for the implementation of 3D-CAD software Rhinoceros.

3.1. Design flow

In the proposed design process, we obtain two compatible states, A and B, which guarantee the compatible deployment motion from A to B. The design flow is as follows (Figure 5).

1. Input a target curved surface (initial of state B) and divide the surface into a quadrilateral mesh.
2. Create a flat mesh (initial of state A) with the same connection relationship.
3. Using the 3D and 2D shapes created in Step 2 as the initial state, let the member lengths of states A and B be the same.

In Step 1, we constrain the number of units gathered around a vertex to be even. This is because, in a scissors' unit with quadrilateral diagonals, when one edge expands, the neighboring edge shrinks. The scale factors around the quad S_i ($i = 0, 1, 2, 3$) satisfy $S_1, S_3 > 1$ and $S_2, S_0 < 1$ (or its opposite). The initial surface division affects the final result, as discussed in Section 3.2..

In Step 2, a simple rectangular grid can be used if the original mesh is a regular quadrilateral mesh.

For Step 3, we created a dynamic relaxation model in which the bars were defined as springs and minimized the potential energy as follows (Figure 6). Here,[] are the names of the goals in Kangaroo2.

Linear Spring (Between A and B) Ensure that identical bars are the same length in the two states. At the same time, set a minimum length to prevent the bar from getting too short. [Equal Length, Clamp Length]

Angle spring 1 (For both A and B) Keep the scissors members in a straight line . [Angle]

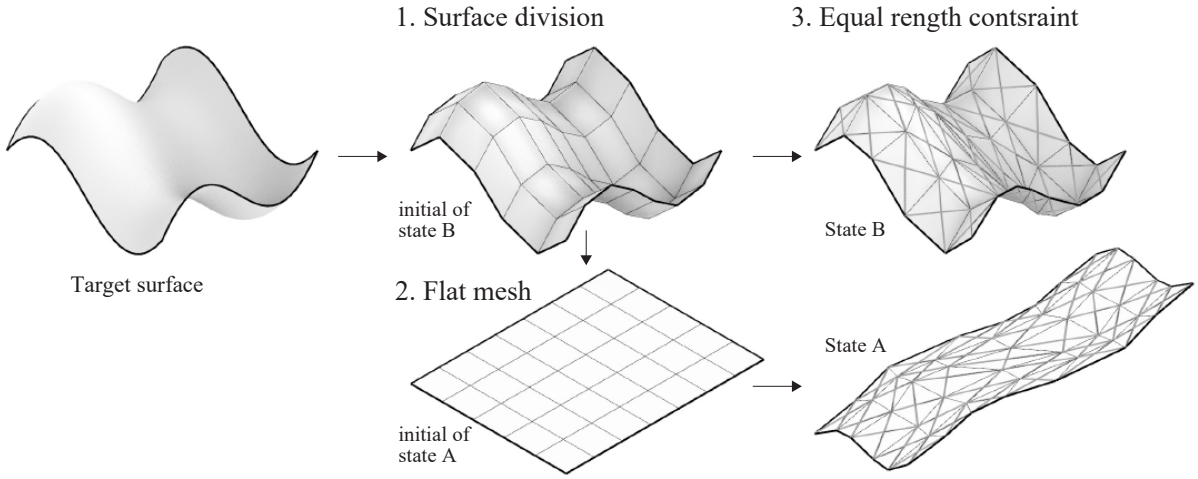

Figure 5: Design flow.

Angle spring 2 (For both A and B) Keep the fold angles between each mesh face (represents the out-of-plane stiffness). [Hinge]

Anchor (For state A) Constrain the vertices of the 2D State on the plane. (For state B) Constrain the internal vertices of the unit connection on the target surface and the exterior vertices on the boundary curve. [On Mesh, On Curve, On Plane]

We set the Linear springs, Angle spring 1, and Anchor on 2D plane hard constraints (with high stiffness) and the other springs soft constraints (with lower stiffness).

Here, Angular Spring 1 constrains the original quadrangular face of the mesh to be planar. This condition is overconstraining as each face does not need to be planar in reality. In actual material, the members can bend in the out-of-plane direction while keeping it geodesically straight on the surface. Geometric constraints to achieve geodesic straightness is still a future work of this study.

3.2. Effect of surface division

The method does not always result in good convergence, depending on the target geometry, parameters of constraints, and initial surface division. Empirically, we found that better convergence solutions were obtained when the target surface was divided into quadrilaterals that were long in one direction in Step 1. This can be attributed to the property of the scissors' units that extend in one direction and contract in the orthogonal direction. The larger the scale factor of the unit's edges, the larger the range of achievable sector angles around the vertex. If the quadrilaterals in the 3D state are long in one direction, a larger edge scaling can be achieved by extending the flat shape in the opposite direction. This enables the larger range of increasing or decreasing sector angles of the unit around the vertex to form a larger family of three-dimensional shapes. In contrast, if the quadrilaterals in the 3D state have nearly square proportions, it may not be possible to ensure a sufficient edge scale factor to reproduce the shape of the target.

To verify this hypothesis, we examined the influence of surface division shape in Step 1 of the method on the results by comparing design results using different proportions of quadrilaterals in the 3D state. Figure 7 shows the results of designing the same target surface with varying numbers of divisions: (a) 5×5, (b) 5×7, and (c) 5×10. While (b) and (c) converged with a 2D shape extending in one direction, (a) failed to converge, with the corner units completely folded in the 2D state.

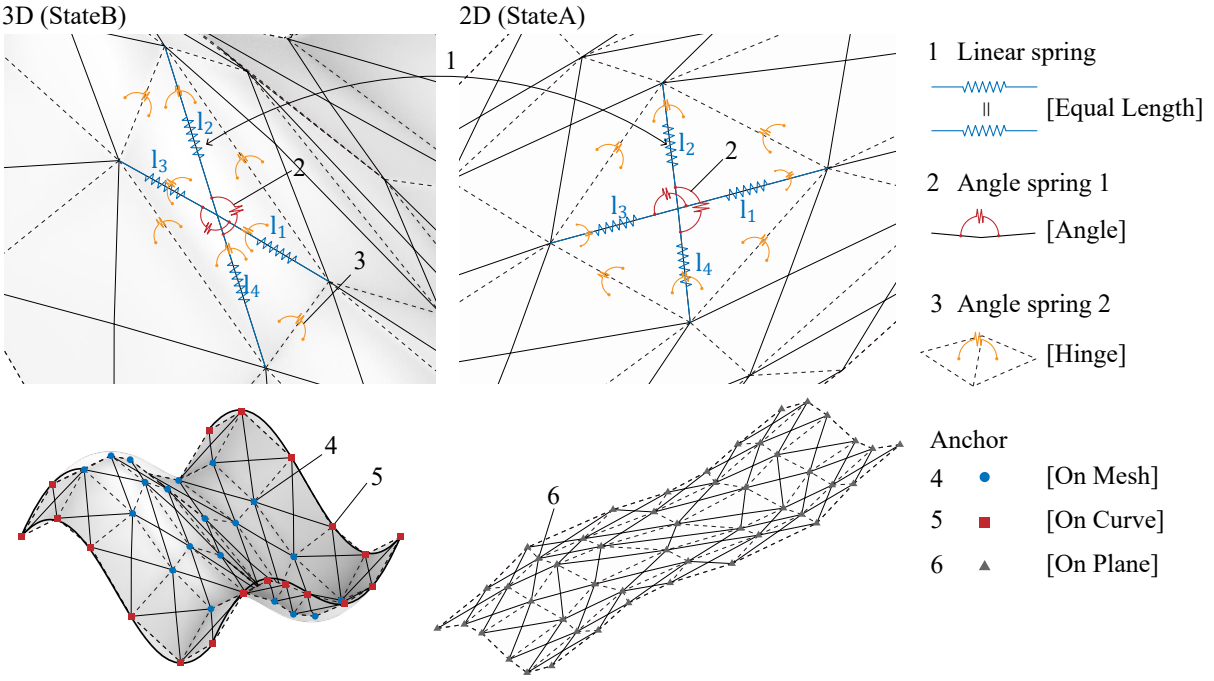

Figure 6: Constraints in Step 3 of the design method.

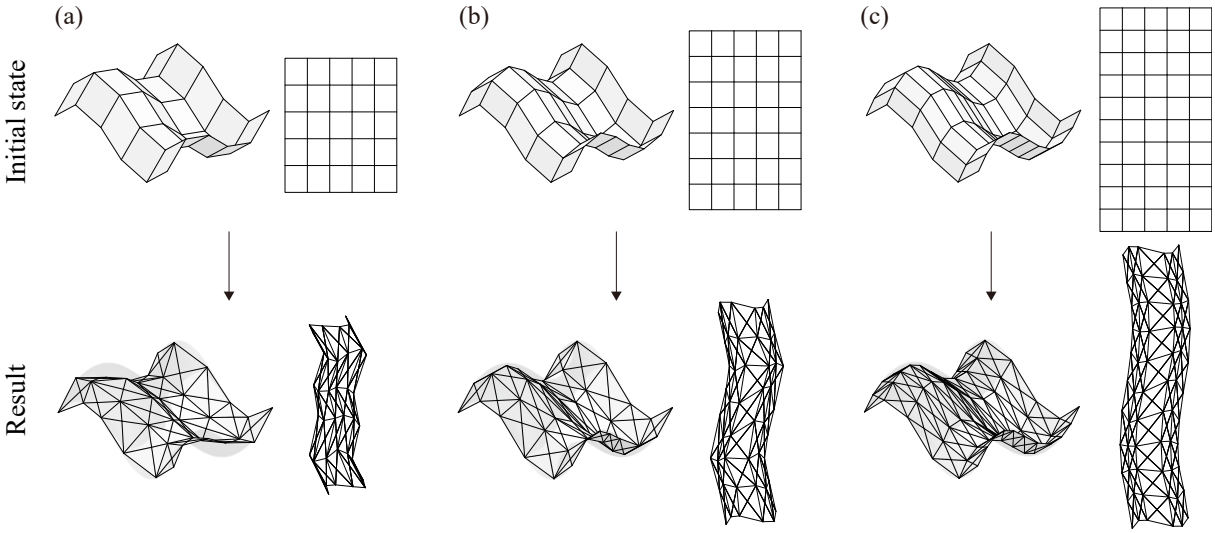

Figure 7: Comparison of the effect of different proportions of quadrilateral segmentation on convergence results. Top: initial state, bottom: results. (a) 5×5, (b) 5×7, (c) 5×10.

4. Design examples and fabrication

4.1. Design and fabrication

We designed mechanisms using the method of Section 3. and created physical models. Figure 9 shows examples of the input surfaces, the design results in 3D and 2D states, and the physical models.

As target surfaces, we used translational surfaces for A to C, revolutional surfaces for D, and a monkey saddle-like surface for E. For model D, as constraints during optimization, a weak constraint to keep them in their initial position ([Anchor]) was applied to the vertices of the units instead of [On Curve] and [On Mesh]. The model E has a 6-fold vertex at the center. We generated the initial quadrilateral mesh for model E by dividing the target surface into six regions and dividing each of them by a quadrilateral grid. All models converged to provide the flat pattern in 2D using our proposed computational approach.

The fabrication process is as follows. First, offset the scissors members in the 2D state by a certain width and make circular holes for pivot hinges at the endpoints and crosspoints to generate the member shape (Figure 8(a)). Here, the scissors member in the 2D state obtained by the design method is not perfectly straight and has kinks at a small angle at the crosspoints. From the viewpoint of ease of fabrication, the member shape was determined by modifying it to a straight line of the same length. The members are cut out of the sheet material using a laser cutter. The parts are managed by giving them numbers and engraving them. This time, the width of the member was $14\,\mathrm{mm}$ and the holes were $5\,\mathrm{mm}$ in diameter for all models. We used $1\,\mathrm{mm}$ or $0.75\,\mathrm{mm}$ thick polypropylene sheets as the members.

For pivot hinges, we used plastic screws at the points where the four sheets come together and eyelets at the crossing points of the scissors (Figure 8(b)).

4.2. Results and discussion

Manufactured mechanisms could be deployed to reproduce a shape close to the target surface.

It was observed that the shapes after deployment for all models, particularly for models B and C, were less curved than the target shapes. This could be caused by the difference in computational models that allow free rotation between units and the physical models that transfer out-of-plane bending between units. The elasticity of the material against out-of-plane bending causes the material to return to a flat surface. Generating a model that takes into account the elasticity of the member is a future work.

In addition, only in-plane curvature can be programmed by this mechanism, and the target shape of the design is not necessarily the equilibrium shape after the physical model is deployed. For example, the saddle-shaped model (Figure 9 C) was stable with the direction of the principal curvature shifted 45 degrees from the target. We believe that this is because the strain energy due to the bending of the member is the smallest in that direction. Fixing the boundary is effective in reproducing the targeted out-of-plane deformation.

5. Conclusion

This paper presented the principles of transformation and a design approach for transformable curved surface mechanisms that combine elastically deformable scissors units. We believe that this research can be applied to deployable shelters and curved formwork structures. In addition, since it can be assembled in a flat state and later deployed, it offers the advantage of constructing free-form curved structures accessible to users without specialized skills. We also anticipate its applicability in product design and artistic endeavors. In the future, we would like to work on structural analysis under load-applied conditions to apply the mechanism to architectural structures.

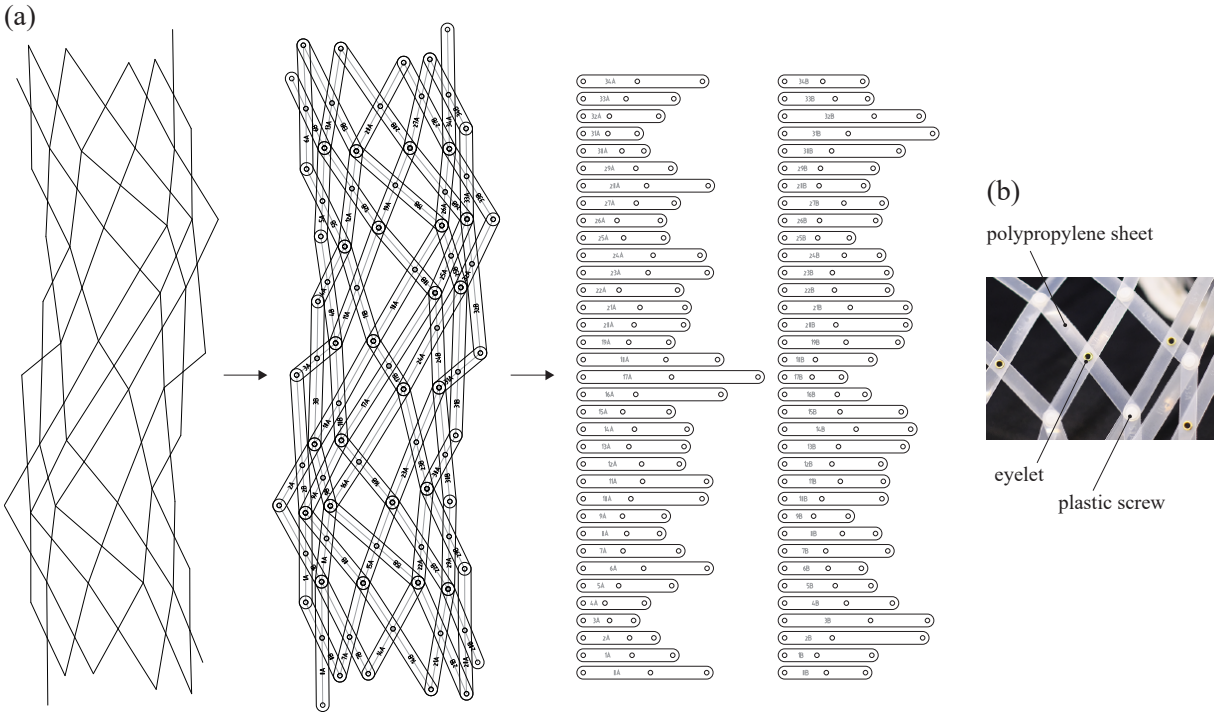

Figure 8: (a) Cut line generation, (b) detail of physical model.

Acknowledgments

This work was supported by JST AdCORP "Realization of people- and environment- friendly artifacts by leveraging computational design and fabrication" and JSPS KAKENHI 22H04954.

References

[1] S. Pillwein, K. Leimer, M. Birsak, and P. Musialski, "On elastic geodesic grids and their planar to spatial deployment," *ACM Transactions on Graphics*, vol. 39, p. 125, Jul. 2020. DOI: 10.1145/3386569.3392490.

[2] J. Panetta, M. Konaković-Luković, F. Isvoranu, E. Bouleau, and M. Pauly, "X-shells: A new class of deployable beam structures," *ACM Transactions on Graphics*, vol. 38, pp. 1–15, Jul. 2019. DOI: 10.1145/3306346.3323040.

[3] Fuki Ono and Tomohiro Tachi, "Growth deformation of surface with constant negative curvature by bending-active scissors structure," *Proceedings of IASS 2022*, 2022.

[4] S. Nishimoto and T. Tachi, "Transformable surface mechanisms by assembly of geodesic grid mechanisms," in *Advances in Architectural Geometry 2023*, K. Dörfler, J. Knippers, A. Menges, S. Parascho, H. Pottmann, and T. Wortmann, Eds. Berlin, Boston: De Gruyter, 2023, pp. 221–234, ISBN: 9783111162683. DOI: doi:10.1515/9783111162683-017. [Online]. Available: https://doi.org/10.1515/9783111162683-017.

[5] Robert McNeel & Associates, *Grasshopper 3d*, https://www.grasshopper3d.com/.

[6] D. Piker, *K2Goals*, https://github.com/Dan-Piker/K2Goals.

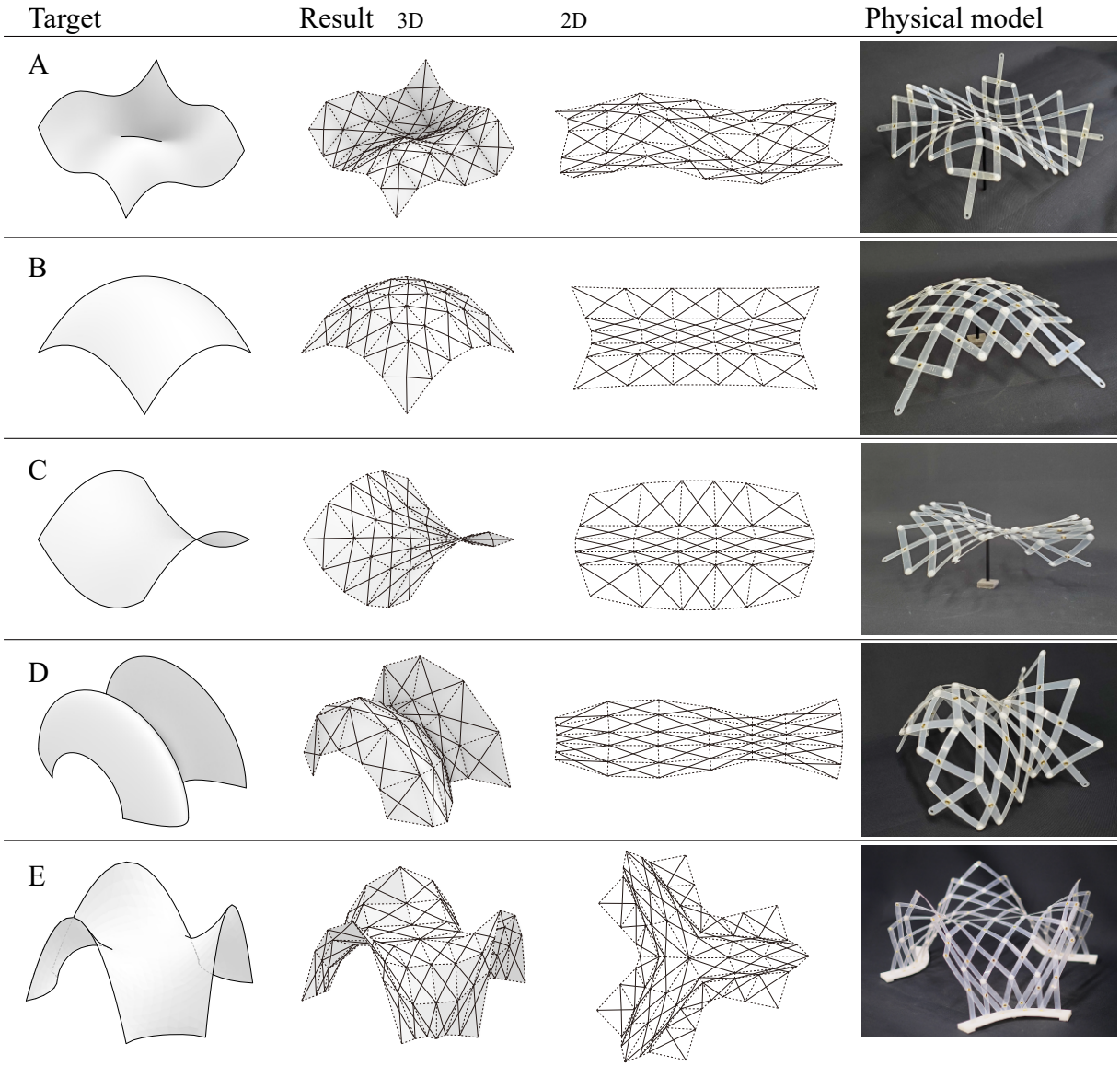

Figure 9: Design examples.